

Structural Characterization of Clusters Formed from Alkyl Nitriles and the Methyl Cation

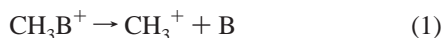
Jeff W. Denault,[†] Feng Wang,[‡] R. Graham Cooks,^{*,†} Fabio C. Gozzo,[§] and Marcos N. Eberlin[§]*Department of Chemistry, Purdue University, West Lafayette, Indiana 47907-1393, Triangle Pharmaceuticals, Durham, North Carolina 27707, and Institute of Chemistry, State University of Campinas, CP 6154 Campinas SP 13083-970, Brazil**Received: June 16, 2000; In Final Form: September 26, 2000*

Cluster ions composed of the alkyl nitriles, acetonitrile (CH₃CN) and butyronitrile (C₃H₇CN), and the methyl cation (CH₃⁺) have been examined in an effort to study methyl cation affinities and the intrinsic nucleophilicity of these bases. Structural characterization of the gas-phase dimeric adduct ions was achieved via multiple stage mass spectrometry (MSⁿ) experiments and by quantum mechanical calculations. The kinetic method was used as a diagnostic tool in determining the structure of the dimeric adduct: the results of tandem mass spectrometry (MS²) experiments are found to provide ratios which exclude loosely bonded dimers based on the thermochemistry of the constituent monomers, and which are consistent with a mixture of noninterconverting covalently bonded structures predicted by ab initio calculations. These clusters are bound such that one nitrile is *N*-methylated and the second nitrile is bound covalently to the carbon of the methylated cyano group. Collision-induced dissociation of this cluster ion results in the loss of a single neutral nitrile whereas both *N*-methylated nitriles should be formed upon dissociation of a loosely bound dimer with the greater fragment ion abundance corresponding to the nitrile having the higher CH₃⁺ affinity. Ab initio calculations show a large barrier between the two isomeric forms of the dimeric cluster and this precludes intramolecular methyl cation transfer between the nitriles. The effects of fluorine substitution at the methyl cation, i.e., CH₂F⁺ and CF₃⁺, on the adducts of the nitriles greatly affects the stability order of the methylated nitrile monomers and dimeric adducts, and thus the abundance ratios of the MS/MS fragments. As the number of fluorine atoms in the cation is increased, the methylated nitrile becomes less stable relative to the dimeric cluster ion.

Introduction

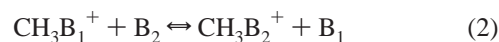
Methylation of organic molecules is important to a wide range of research areas where bimolecular methyl transfer reactions (cationic S_N2 reactions) occur, e.g., interstellar molecular synthesis,¹ organic synthesis using diazonium ions² or halonium ions,³ and the carcinogenic potency of alkylating agents.⁴ Gas-phase studies of ionic methylation have recently been focused on the determination of methylation sites of biomolecules with multiple basic sites.^{5–9} While the site of gas-phase protonation of polyfunctional molecules generally follows trends in proton affinity (N > S > O), the site of attachment for alkyl ions (e.g., CH₃⁺) is often under kinetic control and follows the nucleophilicity order (S > N > O).¹⁰ Analytical applications of methylation reactions include the characterization of oligonucleotides: the gas-phase fragmentation of oligonucleotides methylated at the guanine site yields the position of the guanine moiety within the oligonucleotide.¹¹

Methyl cation affinities (MCAs) defined as the enthalpy change for reaction 1,



are known to correlate directly with proton affinity (PA).^{12,13} Analogous to the determination of proton affinities via measure-

ments of proton transfer equilibria, methyl cation affinities have been determined experimentally from methyl cation transfer equilibrium involving pairs of bases, B₁ and B₂.



To a limited extent, relative MCAs have been determined by equilibrium studies using either ion cyclotron resonance (ICR) mass spectrometry or high-pressure mass spectrometry.^{13–16} However, because the methyl transfer reaction is usually slow and reaches equilibrium at long times, MCAs have often been determined by measuring enthalpies of formation.

In contrast to the extensive studies involving negative reactant ions,^{17–28} gas-phase S_N2 reactions involving positive reactant ions have received little attention, partly because substitution is observed only when the reaction is exothermic and proton transfer from the substrate to the nucleophile is endothermic. Although front-side attack at the reaction center has been proposed in some cases,^{14,29,30} backside attack is the favored mechanism and the reaction coordinate for the gas-phase cationic S_N2 reaction takes the form of the double-well potential energy surface.^{17,31–33}

The dissociation kinetics of cluster ions bound through a central charged moiety can be used to make quantitative estimates of thermochemical properties of the ligands, provided certain assumptions regarding the cluster structure and the dissociation energetics hold.^{34–38} Briefly, the underlying principle of this method, known as the kinetic method, can be

* Author for correspondence: cooks@purdue.edu.

† Purdue University.

‡ Triangle Pharmaceuticals.

§ State University of Campinas.

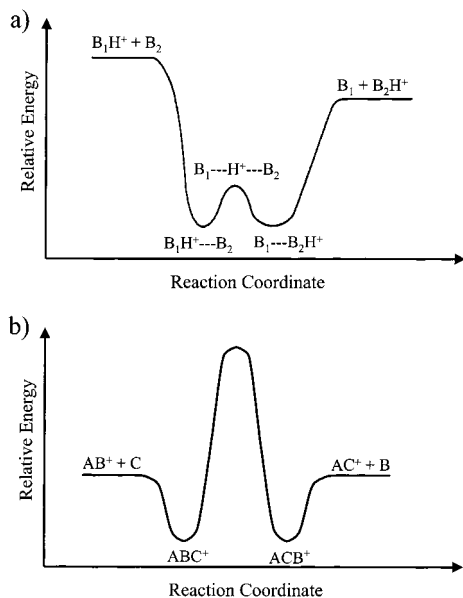
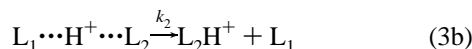
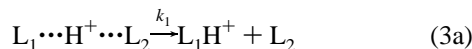


Figure 1. (a) Double well potential energy surface for a proton-bound dimer. (b) Double well potential energy surface for two noninterconverting isomeric structures.

illustrated by the unimolecular dissociation of a proton-bound dimer, $L_1 \cdots H^+ \cdots L_2$, shown in eq 3,



where k_1 and k_2 are the rate constants for the competitive dissociations of the cluster ion to yield $L_1 H^+$ and $L_2 H^+$, respectively. For such a system, a double-well potential energy surface, as shown in Figure 1a, is applicable. The barrier for interconversion between the two isomeric structures is low compared to the dissociation threshold and the two structures are in equilibrium prior to dissociation. Further, for simple bond cleavages, the reverse activation energy is negligible. With the assumptions of negligible entropy differences, negligible reverse activation barriers, and rapid interconversion between the two isomeric structures, the dissociation kinetics reflect the differences in the enthalpy values associated with each dissociation channel. That is to say, the logarithm of the ratio of the two competitive dissociation rates, measured as the ratio of the fragment ion abundance, $[L_1 H^+]/[L_2 H^+]$, is directly proportional to the proton affinity difference between the two ligands as shown in

$$\ln(k_1/k_2) = \ln([L_1 H^+]/[L_2 H^+]) \cong \Delta(\Delta H)/RT_{\text{eff}} = \Delta PA/RT_{\text{eff}} \quad (4)$$

where T_{eff} is the effective temperature of the activated cluster ion.^{35,36,39,40} Similarly, for the dissociation of a *loosely bound* methyl-cation cluster ion $[L_1 CH_3 L_2]^+$, relative methyl cation affinities can be obtained from

$$\ln(k'_1/k'_2) = \ln([L_1 CH_3^+]/[L_2 CH_3^+]) \cong \Delta(\Delta H(CH_3^+))/RT_{\text{eff}} = \Delta MCA/RT_{\text{eff}} \quad (5)$$

The application of the kinetic method, while not a standard technique for structural characterization, has value as a structural tool for cluster ions in cases where the thermochemistry of the

constituent monomers is known. The fragment ratios obtained from MS/MS experiments can be compared with those expected by the kinetic method or precisely calculated for a proposed structure or a collection of alternative structures. Dissociation of dimeric cluster ions which does not correlate with the appropriate thermochemical quantity means that the structures of the monomeric and the dimeric clusters must be incorrect. In one structural application of the method, Squires and co-workers⁴¹ have taken advantage of the differences in proton affinity of *o*-, *m*-, and *p*-nitrobenzoates to authenticate the structures of *o*-, *m*-, and *p*-benzynes isomers. The benzyne anions synthesized in the gas phase were derivatized to give the appropriate nitrobenzoate. The dissociation of the proton-bound dimer of the respective nitrobenzoate formed with $\text{CHF}_2\text{CO}_2\text{H}$ allowed identification of the isomeric form of the precursor benzyne. Structural features of dimeric clusters have also been determined. Gas-phase agostic bonding in clusters composed of SiCl^+ and ortho-substituted pyridines was identified as a result of an apparent increase in proton affinity of the ortho-substituted pyridines when analyzed by the kinetic method. The increased stability resulting from auxiliary hydrogen bonding between SiCl^+ and the ortho-substituent was observed as a deviation from the expected linear correlation between the proton affinity and the natural logarithm of the branching ratio.⁴²

Collision-induced dissociation of gas-phase ions is a classical method of obtaining structurally diagnostic information based on the observed fragments. By varying the collision energy, one can obtain the energy dependence of the different fragmentation channels of the mass-selected ion. The fragmentation of mass-selected cluster ions can be explained by an appropriate potential energy surface, for which two extreme cases can be illustrated. In the first case, typical of most cation-bound dimer ions, the potential energy surface is the double-well potential energy surface in which the interconversion barrier is much lower than either dissociation threshold (Figure 1a). Regardless of the starting structure(s), at low collision energies the dissociation of the cluster ion favors the pathway which is lower in energy. In the second case, which appears to hold for the methylated dimers studied here, the potential energy surface is again a double-well surface, however, the barrier to interconversion is much larger than that of either dissociation threshold (Figure 1b). In this case, the dissociation channels for the two isolated species are independent of one another and such a surface precludes the use of the kinetic method for thermochemical quantitation.

Yet another important tool for ion structural characterization, isotopic labeling, was also employed in the present study. Isotopic substitution identifies possible rearrangement pathways and kinetic isotope effects indicate which bonds are being broken in the rate-determining step for the dissociation of the ion. Isotope effects on gas-phase ion/molecule reactions have been widely utilized to obtain information regarding ion structure and reaction mechanism.^{43–46} For example, Audier and co-workers⁴⁷ have examined catalyzed keto–enol isomerization of ionized acetophenone using deuterium labeling. Using labeled reactants, the authors show that the bimolecular isomerization of ionized acetophenone proceeds via a 1,3-H transfer while the unimolecular isomerization proceeds via two 1,4-H transfers. Large isotope effects are observed for the catalyzed isomerization when $\text{C}_6\text{H}_5\text{COCD}_3^+$ is converted to $\text{C}_6\text{H}_5\text{C}(\text{OD})\text{CD}_2^+$. In isolated ions, these effects are strongly dependent on ion internal energies and on the entropies of activation. The change of the dissociation rate constant upon isotopic substitution is primarily due to the mass-dependent difference between the vibrational zero-point

energies of the ground state and the activated complex. Large isotope effects are associated with ions of low energy and with activated complexes that fragment by simple bond cleavage.

As a continuation of our interest in thermochemical and structural issues related to cation–ligand bonding, we examine the dimeric clusters composed of CH_3^+ with two nitriles and report on the structure and energetic features of an interesting case in which the kinetic method functions as a key structural diagnostic tool. The effects of fluorine substitution upon the methyl cation and the inversion of monomer and dimer stability upon fluorination will be discussed. Ab initio calculations are made for comparison with the experimental data.

Experimental Section

Collision induced dissociation (CID) and selected ion monitoring (SIM) experiments were performed on a Finnigan TSQ 700 triple quadrupole mass spectrometer (Finnigan MAT, San Jose, CA). For these experiments, iodomethane (CH_3I) was leaked into the ion source through a modified GC inlet via a Granville Philips leak valve, such that an abundance of the methylation reagent ion, $(\text{CH}_3)_2\text{I}^+$, was observed. The nitriles were then leaked into the ion source through the probe inlet via a Granville Philips leak valve. For the CID experiments, the CH_3^+ -bound dimeric adduct formed in the ion source was mass-selected using the first quadrupole (Q1) and activated by collision in the second quadrupole (Q2) with argon at a pressure such that single collisions were ensured (viz. the decrease in the main beam intensity after gas addition was no more than 20%).⁴⁸ The dissociation products of the dimers were mass-analyzed by scanning the third quadrupole (Q3) of the triple quadrupole. Multiple scans were signal averaged for each experiment. Energy-resolved CID experiments were performed at a number of collision energies (collision energy determined by the potential difference between the collision quadrupole and the ion source). For each collision energy, multiple experiments were again performed.

The custom-built pentaquadrupole mass spectrometer is comprised of three mass-analyzing quadrupoles (Q1, Q3, and Q5) and two rf-only collision quadrupoles (Q2 and Q4).⁴⁹ The cluster ions of interest were generated by chemical ionization (CI) of a nitrile mixture introduced into the ion source using iodomethane (CH_3I) as reagent gas at a source temperature of about 135 °C. Iodomethane was introduced via the CI gas line at a nominal pressure of 8×10^{-6} Torr, monitored using an ion gauge located near Q5. The indicated pressure rose to 4×10^{-5} Torr upon addition of a mixture of nitriles via a Granville Philips leak valve (Granville Phillips Co., Boulder, CO), and it increased further to 5×10^{-5} Torr upon addition of argon collision gas to Q4. The attenuation of the ion beam upon introduction of the argon was about 20%, which corresponds to the single collision limit. The dimer of interest was mass selected using Q1, transmitted through Q2 and Q3 operated in a broadband transmission mode and dissociated in Q4 by collision with argon at 10 eV energy. The resulting product ions were mass analyzed by scanning Q5.

All compounds were commercially available (Aldrich Chemical Co., Milwaukee, WI) and used without further purification. Mass-to-charge ratios are reported using the Thomson unit (1 Thomson = 1 Da/unit charge).⁵⁰

Ab initio calculations were performed by standard procedures using the Gaussian 94 set of programs.⁵¹ The geometry of the ions of interest were optimized at the HF/6-311G(d,p) level of theory. MP2/6-311+G(2df, 2p) single point energy calculations were performed for the optimized geometries.

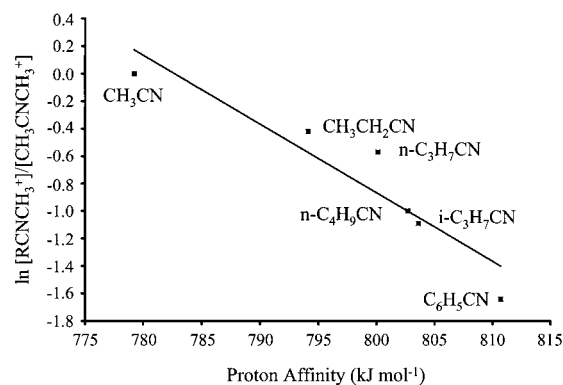


Figure 2. Inverse relationship between the methyl cation affinity and the proton affinity of the reference bases for dissociation of CH_3^+ alkyl nitrile adducts plotted as the logarithm of the ratio of abundances of the methylated monomers $\ln [\text{RCNCH}_3^+]/[\text{CH}_3\text{CNCH}_3^+]$ against the proton affinity of the reference base.

Results and Discussion

Our interest in the structural characterization of cluster ions composed of two alkyl nitriles and the methyl cation stems from the apparent inconsistency between the collision-induced dissociation results for this system, when compared to the results obtained for other polyatomic cations. In previous work with other polyatomic cations, such as OCNCO^+ , SiF_3^+ , PCl_2^+ , and NO^+ ,^{52–55} a linear correlation was observed between the polyatomic cation affinity and the proton affinity of the reference bases. In these cases, the data can be analyzed by the kinetic method and are consistent with loosely bound dimeric clusters. Collision-induced dissociation experiments of a series of cluster ions composed of two nitriles and the methyl cation were performed under single collision conditions with argon and at a translational energy of 10 eV (laboratory frame). The results, do not show the expected linear correlation between the branching ratios of the methyl cation cluster and the proton-bound cluster. Instead a roughly inverse correlation between the two thermochemical quantities is seen, as shown in Figure 2. Note that a stair-step method was used to obtain log ratio values relative to CH_3CN . As noted in the Introduction, the competitive dissociation of a proton-bridged dimer results in two protonated monomers and the logarithm of the abundance ratio is linearly related to the proton affinity difference of the two bases, a result which forms the basis for the kinetic method of estimating proton affinity values.^{35–37,56} For the previously mentioned cation-bound dimers, the ligands are bound symmetrically around the cation of interest. The results obtained in the present study suggest that the nitriles are not symmetrically bound to the methyl cation since it is well-established that methyl cation affinities do correlate with proton affinities of a large number of bases.¹⁵

To better understand the structure and dissociation behavior of the methyl cation/nitrile cluster ions, energy-resolved collision-induced dissociation experiments were performed on a model system, the cluster ion composed of the methyl cation, acetonitrile and butyronitrile. The dissociation of the cluster ion yielded two fragments having mass-to-charge 56 Th and 84 Th, corresponding to the individual methylated monomers. The branching ratio of the product ion abundance, $[\text{CH}_3\text{CN}\cdots\text{CH}_3^+]/[\text{C}_3\text{H}_7\text{CN}\cdots\text{CH}_3^+]$, was determined to have a small energy dependence, as shown in Figure 3. Note that the measured branching ratio is simply the ratio of two product ions observed in the dissociation of a population of mass-selected ions, which here may include structural isomers. It is interesting to note that in this particular data set the methylated butyronitrile, C_3H_7-

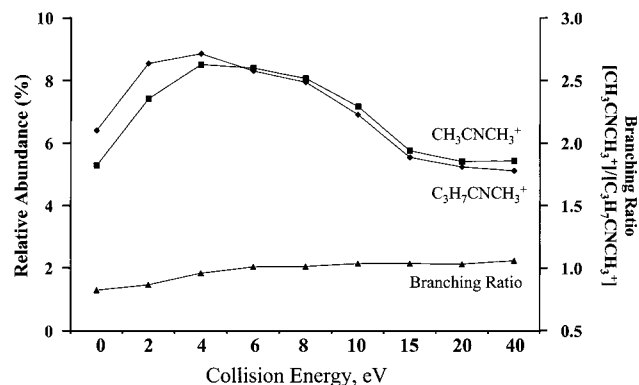


Figure 3. Collision energy dependence of the product ion intensity for the unimolecular dissociation of the cluster ion, $[\text{CH}_3\text{CN}\cdots\text{CH}_3^+\cdots\text{C}_3\text{H}_7\text{CN}]$: (■) $\text{CH}_3\text{CNCH}_3^+$; (◆) $\text{C}_3\text{H}_7\text{CNCH}_3^+$; (▲) $\text{CH}_3\text{CNCH}_3^+/\text{C}_3\text{H}_7\text{CNCH}_3^+$.

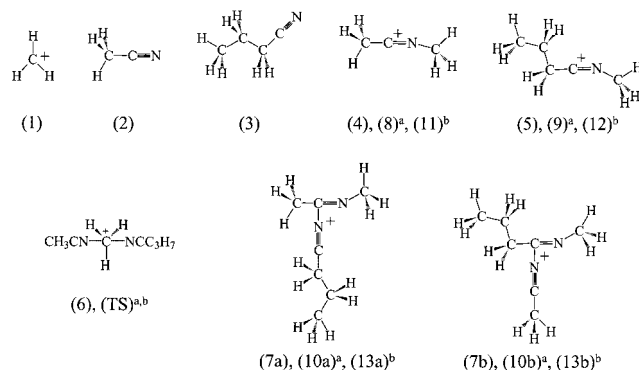


Figure 4. Structures of the reactants, monomers, and dimers for the CH_3^+ , CH_3CN , and $\text{C}_3\text{H}_7\text{CN}$ system (formal charge indicated). ^aStructure numbers for the corresponding CH_2F^+ clusters. ^bStructure numbers for the corresponding CF_3^+ clusters.

CNCH_3^+ , which is the thermodynamically favored product, is more abundant at collision energies below 8 eV (laboratory frame), while the alternative product, methylated acetonitrile ($\text{CH}_3\text{CNCH}_3^+$), is more abundant at higher collision energies. From the methyl cation affinities of acetonitrile and butyronitrile, $\text{MCA}(\text{C}_3\text{H}_7\text{CN}) = 101 \text{ kcal mol}^{-1}$, $\text{MCA}(\text{CH}_3\text{CN}) = 98 \text{ kcal mol}^{-1}$,¹³ a product ion abundance ratio greater than unity is expected, viz. the low collision energy result is expected. A more detailed discussion of the branching ratio will be given below.

Ab initio calculations performed on the model system, $[\text{CH}_3\text{CN}/\text{C}_3\text{H}_7\text{CN}/\text{CH}_3^+]$, provide key information regarding the structure and dissociation thermodynamics of the methyl cation clusters of nitriles. The structures and energies, calculated at the $\text{MP2}/6\text{-}311+\text{G}(2\text{df},2\text{p})//6\text{-}311\text{G}(\text{d},\text{p})$ level, for the reactants, methylated monomers, and dimers are given in Figure 4 and Table 1, respectively. The energies calculated for the methyl cation, acetonitrile and methylated acetonitrile are in good agreement with those calculated by Smith et al. in their study of the association reaction of CH_3^+ with CH_3CN .⁵⁷

Methylation of the nitriles occurs at the nitrogen and leads to the formation of an iminium ion where the positive charge is delocalized over the cyano group.⁵⁸ Simply on the basis of charge stabilization, one would anticipate butyronitrile to have a higher methyl cation affinity than acetonitrile. This is indeed the case as the calculated methyl cation affinity of butyronitrile is $3.5 \text{ kcal mol}^{-1}$ higher than that of acetonitrile.

The potential energy surface for the methyl transfer reaction between acetonitrile and butyronitrile, calculated at the level

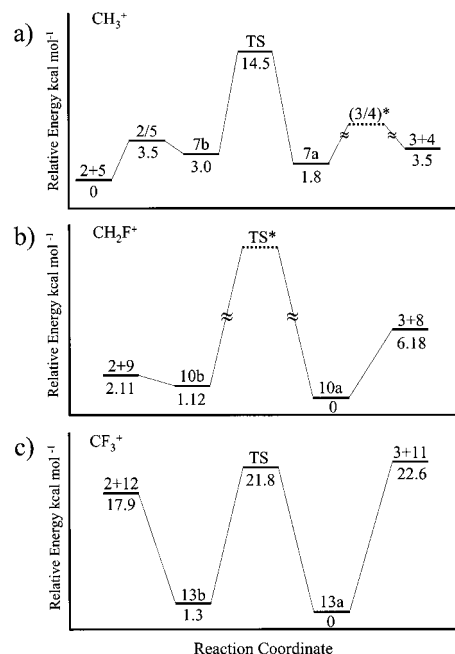


Figure 5. Potential energy surface for methyl transfer reaction between acetonitrile and butyronitrile calculated at the level of $\text{MP2}/6\text{-}311+\text{G}(2\text{df},2\text{p})//6\text{-}311\text{G}(\text{d},\text{p})$. (a) CH_3^+ transfer (b) CH_2F^+ transfer, and (c) CF_3^+ transfer. *Transition state not calculated.

TABLE 1: MP2/6-311+G(2df,2p)//6-311g(d,p) and Zero Point Energies for the Reactants, Monomers, and Dimers for the CH_3CN , $\text{C}_3\text{H}_7\text{CN}$, and CH_3^+ System

structure	energy (Hartrees)	zero point energy (kcal mol^{-1})	
1	CH_3^+	-39.37399	20.77
2	CH_3CN	-132.47709	30.32
3	$\text{C}_3\text{H}_7\text{CN}$	-210.91186	68.50
4	$\text{CH}_3\text{CNCH}_3^+$	-172.01494	56.86
5	$\text{C}_3\text{H}_7\text{CNCH}_3^+$	-250.45534	95.02
6	$\text{CH}_3\text{CNCH}_3 + \text{NCC}_3\text{H}_7$	-382.90926	
7a	$\text{CH}_3\text{C}^+(\text{NCC}_3\text{H}_7)\text{NCH}_3$	-382.92947	
7b	$\text{C}_3\text{H}_7\text{C}^+(\text{NCC}_3\text{H}_7)\text{NCH}_3$	-382.92763	

$\text{MP2}/6\text{-}311+\text{G}(2\text{df},2\text{p})//6\text{-}311+\text{G}(\text{d},\text{p})$, is shown in Figure 5a. (Ion/dipole complexes are not shown.) Interestingly, the expected loosely bound dimer, **6**, that would allow for methyl cation affinity measurements is not a minimum on the surface; it collapses to give the stable, covalently bound species, **7a** and **7b**. The most dramatic difference between the potential energy surface calculated for this reaction and the potential energy surface for the proton-transfer reaction in a proton-bound cluster, as shown in Figure 1a, is the large barrier to interconversion between the two activated cluster ions. Because of the magnitude of the barrier, $\sim 12 \text{ kcal mol}^{-1}$, the two complexes are expected to be stabilized by collisions and isolated in their respective potential wells. More importantly, because this energy barrier is much higher than the dissociation threshold for formation of the respective reactant complexes, intramolecular methyl transfer between nitriles cannot occur under the experimental conditions employed here. However, intermolecular methyl cation transfer between the dimeric cluster ion and a neutral nitrile in the ion source is certainly not excluded. The intermolecular methyl cation transfer would occur via an $\text{S}_{\text{N}}2$ mechanism and would equilibrate the system. Such a process would slightly favor the formation of the more stable dimer structure, **7a**. Both isomeric complexes, when activated, will yield the precursor monomer and neutral exclusively. The branching ratio at collision energies which allow sufficient dissociation of the second channel (**7a** \rightarrow **3** + **4**), is near unity, suggesting that the populations of the

two dimers, **7a** and **7b**, are formed in equal abundance under the conditions employed for this experiment.

The system is also interesting in that the addition of CH_3CN to $\text{C}_3\text{H}_7\text{CNCH}_3^+$ is an endothermic process whereas the addition of $\text{C}_3\text{H}_7\text{CN}$ to $\text{CH}_3\text{CNCH}_3^+$ is an exothermic process (Figure 5a). This is easily understood taking into account the ability of the second ligand to stabilize the positive charge which is delocalized over the cyano group (C_3H_7 stabilization is better than CH_3 stabilization). The addition of CH_3CN to $\text{C}_3\text{H}_7\text{CNCH}_3^+$ moves the charge to the cyano group of acetonitrile, which stabilizes the charge to a smaller degree than occurs in the initial cluster. During the addition of $\text{C}_3\text{H}_7\text{CN}$ to $\text{CH}_3\text{CNCH}_3^+$, the charge is better stabilized at the cyano group of $\text{C}_3\text{H}_7\text{CN}$ when compared to the initial cluster. The dissociation of cluster, **7b**, occurs over a barrier which is calculated to be $1.5 \text{ kcal mol}^{-1}$ higher than the initial cluster energy. This barrier traps the cluster ions in the potential well and allows them to be isolated for the MS/MS experiment. An equivalent barrier is likely to exist for the dissociation of cluster **7a**, effectively increasing the threshold at which the cluster will dissociate. Charge stabilization and the barrier to dissociation for each of the clusters help explain the energy-resolved CID experiments observed in these experiments. At low collision energies **7b** dissociates more readily than **7a**, a result of the lower relative barrier to dissociation. As the collision energy is raised and approaches the dissociation barrier for **7a**, fragmentation of **7a** begins to compete more favorably with the dissociation of **7b**. Note that each dissociation channel occurs from a distinct reactant ion. Keeping in mind that rapid interconversion of the activated cluster ion is a requirement for affinity determinations by the kinetic method, the potential energy surface given here indicates that the determination of methyl cation affinities for nitriles is not possible by this methodology.

The barrier to interconversion for the potential energy surface proposed for this system suggests that if one could form the cluster from either **3** + **4** or **2** + **5** as opposed to a one-pot synthesis in the ion source, only one product, the original methylated species, would be observed in the ensuing collision-induced dissociation experiment. To test this hypothesis, an MS^3 experiment was performed using the pentaquadrupole mass spectrometer. Acetonitrile was methylated by the dimethylidonium ion in the ion source and the monomer (m/z 56) was mass-selected by the first quadrupole and allowed to react with butyronitrile under multiple collision conditions in the second quadrupole. The dimer (m/z 125) was then mass-selected by the third quadrupole and activated by collision with argon under single collision conditions in the fourth quadrupole. The product ion mass spectrum was obtained by scanning the fifth quadrupole. The resulting mass spectrum, shown in Figure 6b, reveals that the dimer formed in this fashion, does indeed fragment to yield the precursor monomer, methylated acetonitrile, exclusively and does not interconvert to yield the methylated butyronitrile product observed when the dimers are made nonselectively in the ion source. This experiment confirms that interconversion does not take place and is consistent with the calculated potential energy surface.

Further experiments were performed in which the ratio of the two nitriles was varied. For solutions containing butyronitrile:acetonitrile ratios of 1:5, 1:1, and 5:1, the branching ratio obtained over a range of collision energies does not vary significantly. While these conditions may not be sufficient to observe a change, the results obtained support the proposal that the system is equilibrated in the high-pressure ion source.

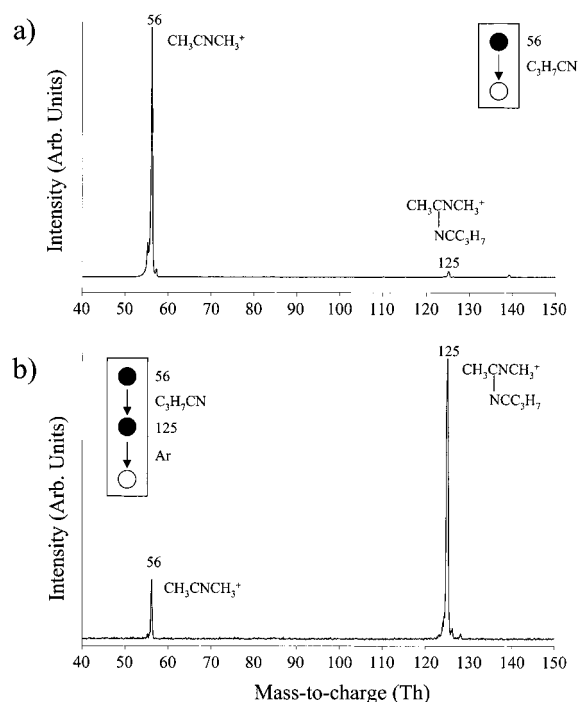


Figure 6. (a) MS/MS product ion spectrum for the formation of the dimer $[\text{CH}_3\text{CN}\cdots\text{CH}_3^+\cdots\text{NCC}_3\text{H}_7]$ (m/z 125). The cluster was formed by mass selecting the methylated acetonitrile, $\text{CH}_3\text{CNCH}_3^+$, in the first quadrupole. (b) MS/MS/MS sequential product ion spectrum for the collision-induced dissociation of the cluster ion formed by mass selecting methylated acetonitrile, $\text{CH}_3\text{CNCH}_3^+$, in the first quadrupole and reacting it with butyronitrile, $\text{C}_3\text{H}_7\text{CN}$, in the second quadrupole.

TABLE 2: Relative Kinetic Isotope Effects

isotopic cation ^a	k_1/k_2^b	$(k_1/k_2)^c$	kinetic isotope effect ^d
$^{12}\text{CD}_3^+$	0.57 ± 0.03	0.22 ± 0.02	2.59 ± 0.27
$^{13}\text{CH}_3^+$	0.57 ± 0.03	0.75 ± 0.03	0.76 ± 0.09

^a Clusters composed of the given cation with acetonitrile and butyronitrile. ^b The branching ratio for the nonlabeled methyl cation measured as $[\text{C}_3\text{H}_7\text{CNCH}_3^+]/[\text{CH}_3\text{CNCH}_3^+]$. ^c The branching ratio for the labeled methyl cation measured as $[\text{C}_3\text{H}_7\text{CNX}^+]/[\text{CH}_3\text{CNX}^+]$, where X is the labeled methyl cation.

Isotopic substitution on CH_3^+ is a further probe of the structure of the dimer structure. The dissociation channels of a cluster ion which is bound asymmetrically with respect to the methyl cation, regardless of the specific structure, would be affected differently upon isotopic labeling of the methyl cation. These differences would give rise to relative kinetic isotope effects which differ from unity. As can be seen from Table 2, the kinetic isotope effects upon deuterium substitution are significantly larger than unity and support the proposal that the dimeric structure is not symmetrically bound about the methyl cation. It is interesting to note that while deuterium substitution results in a *normal* relative isotope effect, ^{13}C labeling of the methyl cation results in an *inverse* relative isotope effect.

In a related study, the effects of fluorine substitution at the methyl cation on the adducts of nitriles was examined.⁵⁹ The potential energy surfaces and the energy resolved mass spectra obtained can be examined in light of the destabilization effects of fluorine. The substituent effects of fluorine on alkyl cations has been examined by Paddon-Row et al.⁶⁰ The replacement of $-\text{CH}_3$ by $-\text{CF}_3$ in the ethyl cation, results in the destabilization of the cation by $37.3 \text{ kcal mol}^{-1}$.⁶⁰ This destabilization can be seen in the nitrile/methyl cation clusters by looking at the potential energy surfaces calculated for the CH_3^+ , CH_2F^+ , and

TABLE 3: Relative Destabilization Effects of Fluorine Substitution

cation	$\Delta E(1)^a$ (kcal/mol)	$\Delta E(2)^b$ (kcal/mol)	av branching ratio ^c
CH ₃ ⁺	3.0	-1.70	0.98
CH ₂ F ⁺	-0.99	-6.18	1.66
CF ₃ ⁺	-16.6	-22.6	2.90

^a Energy difference for the loss of CH₃CN from the respective dimer.

^b Energy difference for the loss of C₃H₇CN from the respective dimer.

^c Branching ratio defined as [CH₃CNCH₃⁺]/[C₃H₇CNCH₃⁺].

CF₃⁺ reactions (Figure 5). The relative destabilization energies of the methylated nitriles compared to the dimeric adduct are given in Table 3. As the number of fluorine atoms in the cation is increased, the methylated nitrile becomes less stable relative to the dimeric cluster ion. This can be understood as the result of the charge being further from the fluorination site in the dimer compared to that of the monomer. This destabilization effect is also apparent when examining the average branching ratio obtained from the energy-resolved CID experiments for the three methyl cation clusters (Table 3). Upon a single fluorine substitution, the branching ratio increases compared to the branching ratio of the CH₃⁺ cluster, indicating an increased preference for the formation of CH₃CNCH₂F⁺ upon dissociation of the adduct, i.e., preferential formation of the species which is less thermodynamically favored. This trend continues upon perfluorination of the methyl cation. In light of the large barrier interconversion between the two isomeric adducts, these results suggest a kinetic effect in the formation of the fluoromethyl cation nitrile adducts which favors the formation of acetonitrile adduct over butyronitrile adduct, consistent with the large barriers shown in Figure 5.

Conclusion

In contrast to the dimeric adduct ions generated from ions such as OCNCO⁺, SiF₃⁺, PCl₂⁺, and NO⁺, the CH₃⁺ adducts do not have symmetrical, loosely bound structures. As a result their fragmentations do not reflect the corresponding cation affinity difference between the two neutral components. While the kinetic method does not provide relative cation affinities, it does provide structural information on the adduct ions. The lack of correlation between the branching ratio and the thermochemical quantity of interest, the methyl cation affinity, is shown to be due to the relatively high interconversion barrier, which prevents internal conversion of the two activated complexes. Therefore, the product ion distribution of the activated clusters results from the combined effects of the bond energy and the composition of the sampled complexes. According to molecular orbital calculations, the most stable structure of methyl cation-bound nitrile dimers involves a neutral nitrile molecule covalently bound to the carbon of the methylated cyano group.

Acknowledgment. This work was supported by the National Science Foundation, CHE 92-23791 and by the FAPESP/CNPq (Brazil). J.W.D. acknowledges a fellowship sponsored by Merck Co. We thank Philip Wong (Bioanalytical Systems, West Lafayette, IN) and Shuguang Ma (Vanderbilt University, Nashville, TN) for experimental assistance and valuable discussions and Randy Julian (Eli Lilly and Co., Indianapolis, IN) for assistance with the ab initio calculations.

References and Notes

- (1) Smith, D.; Adams, N. G. In *Interstellar Molecules*; Andrews, B. H., Ed.; 1980.
- (2) Keating, J. T.; Skell, P. S. In *Carbonium Ions*; Olah, G., Schleyer, P. V. R., Eds.; Wiley-Interscience: New York, 1970.

- (3) Olah, G. A. In *Halonium Ions*; Wiley: New York, 1975.
- (4) Ford, G. P.; Scribner, J. D. *J. Am. Chem. Soc.* **1983**, *105*, 349.
- (5) Wood, K. V.; Burinsky, D. J.; Cameron, D.; Cooks, R. G. *J. Org. Chem.* **1983**, *48*, 5236.
- (6) Burinsky, D. J.; Campana, J. E. *Org. Mass Spectrom.* **1988**, *23*, 613.
- (7) Chowdhury, S.; Harrison, A. G. *Org. Mass Spectrom.* **1988**, *23*, 79.
- (8) Houriet, R.; Rolli, E.; Flammang, R.; Maquestiau, A.; Bouchoux, G. *Org. Mass Spectrom.* **1987**, *22*, 770.
- (9) Attina, M.; Cacace, F.; Ricci, A. *Angew. Chem., Int. Ed. Engl.* **1991**, *30*, 1457.
- (10) Burinsky, D. J.; Campana, J. E. *Org. Mass Spectrom.* **1984**, *19*, 539.
- (11) Marzilli, L. A.; Barry, J. P.; Sells, T.; Law, S. J.; Vouros, P.; Harsch, A. *J. Mass Spectrom.* **1999**, *34*, 276.
- (12) Brauman, J. I.; Han, C. C. *J. Am. Chem. Soc.* **1988**, *110*, 5611.
- (13) Deakynne, C. A.; Meot-Ner, M. *J. Phys. Chem.* **1990**, *94*, 232.
- (14) Holtz, D.; Beauchamp, J. L.; Woodgate, S. D. *J. Am. Chem. Soc.* **1970**, *92*, 7484.
- (15) McMahon, T. B.; Heinis, T.; Hovey, J. K.; Kebarle, P. *J. Am. Chem. Soc.* **1988**, *110*, 7591.
- (16) Glukhovtsev, M. N.; Szulejko, J. E.; McMahon, T. B.; Gauld, J. W.; Scott, A. P.; Smith, B. J.; Pross, A.; Radom, L. *J. Phys. Chem.* **1994**, *98*, 13099.
- (17) Riveros, J. M.; Jose, S. M.; Takashima, K. *Adv. Phys. Org. Chem.* **1985**, *21*, 197.
- (18) Bohme, D. K.; MacKay, G. I. *J. Am. Chem. Soc.* **1981**, *103*, 978.
- (19) McDonald, R. N.; Chowdhury, A. K. *J. Am. Chem. Soc.* **1985**, *107*, 4123.
- (20) Caldwell, G.; Magnera, T. F.; Kebarle, P. *J. Am. Chem. Soc.* **1984**, *106*, 959.
- (21) Depuy, C. H.; Gronert, S.; Mullin, A.; Bierbaum, V. M. *J. Am. Chem. Soc.* **1990**, *112*, 8650.
- (22) Shaik, S.; Ioffe, A.; Reddy, A. C.; Pross, A. *J. Am. Chem. Soc.* **1994**, *116*, 262.
- (23) Graul, S. T.; Bowers, M. T. *J. Am. Chem. Soc.* **1994**, *116*, 3675.
- (24) Glukhovtsev, M. N.; Pross, A.; Radom, L. *J. Am. Chem. Soc.* **1995**, *117*, 2024.
- (25) Brauman, J. I.; Olmstead, W. N.; Lieder, C. A. *J. Am. Chem. Soc.* **1974**, *96*, 4030.
- (26) Olmstead, W. N.; Brauman, J. I. *J. Am. Chem. Soc.* **1977**, *99*, 4219.
- (27) Brauman, J. I. *J. Mass Spectrom.* **1995**, *30*, 1649.
- (28) Craig, S. L.; Brauman, J. I. *Science* **1997**, *276*, 1536.
- (29) Holtz, D.; Beauchamp, J. L. *Nature (London)* **1971**, *231*, 204.
- (30) Beauchamp, J. L.; Caserio, M. C.; McMahon, T. B. *J. Am. Chem. Soc.* **1974**, *96*, 6243.
- (31) Raghavachari, K.; Chandrasekhar, J.; Burnier, R. C. *J. Am. Chem. Soc.* **1984**, *106*, 3124.
- (32) Speranza, M.; Angelini, G. *J. Am. Chem. Soc.* **1980**, *102*, 3115.
- (33) Hall, D. G.; Gupta, C.; Morton, T. H. *J. Am. Chem. Soc.* **1981**, *103*, 2416.
- (34) Cooks, R. G.; Kruger, T. L. *J. Am. Chem. Soc.* **1977**, *99*, 1279.
- (35) McLuckey, S. A.; Cameron, D.; Cooks, R. G. *J. Am. Chem. Soc.* **1981**, *103*, 1313.
- (36) Cooks, R. G.; Patrick, J. S.; Kotiaho, T.; McLuckey, S. A. *Mass Spectrom. Rev.* **1994**, *13*, 287.
- (37) Cooks, R. G.; Wong, P. S. H. *Acc. Chem. Res.* **1998**, *31*, 379.
- (38) Armentrout, P. B. *J. Mass Spectrom.* **1999**, *34*, 74.
- (39) Drahos, L.; Vekey, K. *J. Mass Spectrom.* **1999**, *34*, 79.
- (40) Ervin, K. M. *Int. J. Mass Spectrom.* **2000**, *196*, 271.
- (41) Wenthold, P. G.; Hu, J.; Squires, R. R. *J. Am. Chem. Soc.* **1996**, *118*, 11865.
- (42) Yang, S. S.; Wong, P.; Ma, S. G.; Cooks, R. G. *J. Am. Soc. Mass Spectrom.* **1996**, *7*, 198.
- (43) Levens, K. *Fundamental Aspects of Organic Mass Spectrometry*; Verlag Chemie: Weinheim, 1978.
- (44) Cooks, R. G.; Beynon, J. H.; Caprioli, R. M.; Lester, G. R. Elsevier: New York, 1973.
- (45) Derrick, P. *J. Mass Spectrom. Rev.* **1983**, *2*, 285.
- (46) Kaye, J. A. *Isotope Effects in Gas-Phase Chemistry*; American Chemical Society: Washington, DC, 1992.
- (47) Chamot-Rooke, J.; van der Rest, G.; Mourgues, P.; Audier, H. E. *Int. J. Mass Spectrom.* **2000**, *196*, 385.
- (48) Holmes, J. L. *Org. Mass Spectrom.* **1985**, *20*, 169.
- (49) Schwartz, J. C.; Schey, K. L.; Cooks, R. G. *Int. J. Mass Spectrom. Ion Processes* **1990**, *1*, 101.
- (50) Cooks, R. G.; Rockwood, A. L. *Rapid Commun. Mass Spectrom.* **1991**, *5*, 93.

(51) Frisch, M. J.; Trucks, G. W.; Schlegel, H. B.; Gill, P. M. W.; Johnson, B. G.; Robb, M. A.; Cheeseman, J. R.; Keith, T.; Petersson, G. A.; Montgomery, J. A.; Raghavachari, K. A.-L. M. A.; Zakrzewski, V. G.; Ortiz, J. V.; Foresman, J. B.; Cioslowski, J.; Stefanov, B. B.; Nanayakkara, A.; Challacombe, M.; Peng, C. Y.; Ayala, P. Y.; Chen, W.; Wong, M. W.; Andres, J. L.; Replogle, E. S.; Gomperts, R.; Martin, R. L.; Fox, D. J.; Binkley, J. S.; Defrees, D. J.; Baker, J.; Stewart, J. P.; Head-Gordon, M.; Gonzalez, C.; Pople, J. A. *Gaussian94*; Gaussian, Inc.: Pittsburgh, PA, 1995.

(52) Yang, S. S.; Chen, G.; Ma, S.; Cooks, R. G.; Gozzo, F. C.; Eberlin, M. N. *J. Mass Spectrom.* **1995**, *30*, 807.

(53) Wong, P. S. H.; Ma, S. G.; Yang, S. S.; Cooks, R. G.; Gozzo, F. C.; Eberlin, M. N. *J. Am. Soc. Mass Spectrom.* **1997**, *8*, 68.

(54) Ma, S.; Wong, P.; Cooks, R. G.; Gozzo, F. C.; Eberlin, M. N. *Int. J. Mass Spectrom. Ion Processes* **1997**, *163*, 89.

(55) Cacace, F.; de Petris, G.; Pepi, F. *Proc. Natl. Acad. Sci. U.S.A.* **1997**, *94*, 3507.

(56) Cooks, R. G.; Koskinen, J. T.; Thomas, P. D. *J. Mass Spectrom.* **1999**, *34*, 85.

(57) Smith, S. C.; Wilson, P. F.; Sudkeaw, P.; Maclagan, R. G. A. R.; McEwan, M. J.; Anicich, V. G.; Huntress, W. T. *J. Chem. Phys.* **1993**, *98*, 1944.

(58) de Lijser, H. J. P.; Arnold, D. R. *J. Phys. Chem. A* **1998**, *102*, 5592.

(59) Alvarez, J.; Denault, J. W.; Cooks, R. G. *J. Mass Spectrom.*, in press.

(60) Paddon-Row, M. N.; Santiago, C.; Houk, K. N. *J. Am. Chem. Soc.* **1980**, *102*, 6561.